

## A NEW FINITE ELEMENT FORMULATION FOR COMPUTATIONAL FLUID DYNAMICS: II. BEYOND SUPG\*

Thomas J.R. HUGHES, Michel MALLET and Akira MIZUKAMI\*\*

*Division of Applied Mechanics, Durand Building, Stanford University, Stanford, CA 94305, U.S.A.*

Received 11 June 1985

A discontinuity-capturing term is added to the streamline-upwind/Petrov–Galerkin weighting function for the scalar advection-diffusion equation. The additional term enhances the ability of the method to produce smooth yet crisp approximations to internal and boundary layers.

### 1. Introduction

The streamline-upwind/Petrov–Galerkin concept (SUPG) was introduced by Hughes and Brooks [8, 9]. In these references, and in [2, 3], SUPG has been applied to the linear scalar advection-diffusion equation and the incompressible Navier–Stokes equations. Initiatory attempts at extending SUPG to hyperbolic systems and, in particular, the compressible Euler equations are presented in [12]. SUPG was applied with success to thermally-coupled incompressible Navier–Stokes flows by Argyris, Doltsinis, Pimenta and Wüstenberg [1]. The mathematical analysis of SUPG has been performed by Johnson and his colleagues (see [14–17, 19]). These works also contain novel extensions of the SUPG concept to time-dependent problems and the incompressible Euler and Navier–Stokes equations. A number of papers have already appeared in which the basic SUPG method is applied to various problems involving advective-diffusive phenomena (see, e.g., papers in [4]).

In the context of the linear advection-diffusion equation, SUPG results in superior behavior compared with previously known finite element methods. Optimal or near-optimal, *global* error estimates are obtained for sufficiently smooth exact solutions. For exact solutions containing sharp internal and/or boundary layers, optimal, or near-optimal, *local* error estimates, valid outside a small neighborhood containing the layers, are attained. Numerical experiences are in conformance with the results of the theoretical error analysis (see the papers of Hughes and Brooks, and Nävert's thesis). The SUPG method thus represents the answer to a fundamental problem in numerical analysis, namely, of finding a higher-order accurate method for the advection-diffusion equation which exhibits good stability properties. The behavior of SUPG may be contrasted with formally-accurate central-difference methods

\* This research was sponsored by the NASA Langley Research Center under Grant NASA-NAG-1-361.

During the course of this work Michel Mallet was supported by an IBM Predoctoral Graduate Fellowship and Akira Mizukami was supported by Stanford University and Nippon Kokan K.K.

\*\* Visiting Scholar from Nippon Kokan K.K., Kawasaki, Japan.

and Galerkin finite element methods for which the presence of sharp layers typically creates globally-propagating oscillations. For these methods no local error estimates are possible. The good stability of SUPG is not accompanied by deterioration of convergence rate, a phenomenon plaguing classical upwind methods which are at best first-order accurate.

Despite the success of SUPG it is no panacea. For example, SUPG does not preclude overshooting and undershooting about sharp layers. In certain applications, oscillatory approximations to layers cannot be permitted and thus methods exhibiting even stronger stability properties (e.g., ‘monotonicity’) are often employed. Monotone methods are described in the monograph of Ikeda [13] (frequently the terminology ‘maximum-principle satisfying methods’ is also used). See also [7, 10, 20]. Monotone methods are often based upon *ad-hoc* constructions and frequently engender shortcomings such as violation of global conservation of flux. Tabata’s method, described in [13], is an example of a monotone method which is not conservative. Until recently, a monotone method for the advection-diffusion equation which simultaneously exhibited global conservation and satisfied the requirements of the Petrov–Galerkin method (i.e., that the exact solution identically satisfies the variational equation of the discrete method) did not exist. This situation was rectified by the method developed by Mizukami and Hughes [18] for three-node triangles. It is well known that *linear* monotone methods can be at most first-order accurate. The method of Mizukami and Hughes is *nonlinear* and superior accuracy is achieved in practice. Unfortunately, it is not clear how to generate higher-order-element counterparts of this method and extension to more complicated situations, such as compressible flows, is not apparent.

The inability to produce non-oscillatory approximations of boundary and interior layers is a main shortcoming of SUPG. In addition, in our opinion, SUPG has not yet attained its canonical generalization to systems. For example, the formulation presented in [3] for the incompressible Navier–Stokes equations has proven reliable in practice. However, simplifications are present in this formulation due to the use of constant-pressure elements. The extension to nonconstant-pressure interpolations is formally straightforward, but raises basic mathematical question (see [17]). Alternative SUPG-type procedures proposed by Johnson and Saranen [17] circumvent the mathematical difficulties but involve other inconveniences, such as either the use of stream function and vorticity as dependent variables, or the necessity of employing discrete velocity fields which exactly satisfy the incompressibility constraint. In addition, generalizations of SUPG to multidimensional hyperbolic systems proposed so far have manifested shortcomings. For example, consider a one-dimensional, diagonalizable, linear system. Application of the methods proposed in, for example, [11, 16] to the coupled system does not even agree with application of the same methods to the uncoupled modal equations.

This is the first of several papers which take SUPG as a starting point and endeavor to systematically generalize it and improve upon its performance in a variety of flow problems. In this paper we consider the multidimensional linear scalar advection-diffusion equation. After reviewing the semidiscrete version of SUPG in Section 2, in Section 3 we describe a simple means for improving resolution of sharp layers while maintaining rate of convergence. The new method involves an additional ‘discontinuity-capturing’ term in the weighting function which has a form similar to the streamline term, but acts in the direction of the solution gradient rather than in the direction of the streamline. The dependence of this term on the solution gradient results in a discrete method which is *nonlinear*. Numerical results which

illustrate significant improvement over SUPG on problems involving sharp layers are presented in Section 4. The new method does not quite attain the precision of the Mizukami–Hughes scheme, but possesses the *crucial* attribute of being generalizable to complex multidimensional systems. Conclusions are drawn in Section 5. The next two papers in this series deal with the generalization of the streamline and discontinuity-capturing operators to systems.

## 2. Review of SUPG

### 2.1. The advection-diffusion equation

Consider the advection-diffusion (AD) equation in  $n_{sd}$  space dimensions:

$$\varphi_t + \mathbf{a} \cdot \nabla \varphi = \nabla \cdot (\boldsymbol{\kappa} \nabla \varphi) + f, \quad (1)$$

where  $\varphi = \varphi(\mathbf{x}, t)$  is the dependent variable, a scalar-valued function of the spatial coordinates  $\mathbf{x} \in \Omega \subset \mathbb{R}^{n_{sd}}$  and time  $t \in ]0, T[$ , where  $T > 0$ . The velocity vector field is denoted  $\mathbf{a} = \mathbf{a}(\mathbf{x})$  and the diffusivity tensor is  $\boldsymbol{\kappa} = \boldsymbol{\kappa}(\mathbf{x})$ . We shall assume for simplicity that  $\boldsymbol{\kappa}$  is isotropic and positive-definite. Therefore  $\boldsymbol{\kappa} = \kappa \mathbf{I}$ , where  $\mathbf{I}$  is the identity tensor, and the scalar  $\kappa = \kappa(\mathbf{x})$  is positive. The given body source term is denoted  $f = f(\mathbf{x}, t)$ .

The boundary of  $\Omega$  is denoted  $\Gamma$ . We assume  $\Gamma$  is decomposed as follows:

$$\Gamma = \overline{\Gamma_g \cup \Gamma_h}, \quad (2)$$

$$\emptyset = \Gamma_g \cap \Gamma_h. \quad (3)$$

We allow both Dirichlet and Neumann (i.e., diffusive flux) boundary conditions, respectively:

$$\varphi(\mathbf{x}, t) = g(\mathbf{x}, t), \quad \forall \mathbf{x} \in \Gamma_g, \quad t \in ]0, T[, \quad (4)$$

$$\mathbf{n}(\mathbf{x}) \cdot \boldsymbol{\kappa}(\mathbf{x}) \nabla \varphi(\mathbf{x}, t) = h(\mathbf{x}, t), \quad \forall \mathbf{x} \in \Gamma_h, \quad t \in ]0, T[, \quad (5)$$

where  $\mathbf{n}$  is the unit outward normal vector to the boundary and  $g$  and  $h$  are prescribed functions.

The initial condition is

$$\varphi(\mathbf{x}, 0) = \varphi_0(\mathbf{x}), \quad \mathbf{x} \in \Omega, \quad (6)$$

where  $\varphi_0$  is a given function. The object of the initial-boundary-value problem is to find  $\varphi = \varphi(\mathbf{x}, t)$ ,  $\mathbf{x} \in \bar{\Omega}$  and  $t \in ]0, T[$ , satisfying (1) and (4)–(6).

### 2.2. Semidiscrete SUPG

Consider a finite element discretization of  $\Omega$  consisting of  $n_{el}$  element domains such that

$$\bar{\Omega} = \bigcup_{e=1}^{n_{el}} \bar{\Omega}^e, \quad (7)$$

$$\emptyset = \bigcap_{e=1}^{n_{el}} \Omega^e. \quad (8)$$

The boundary of  $\Omega^e$  is denoted  $\Gamma^e$ . The interior boundary is defined to be

$$\Gamma_{\text{int}} = \bigcup_{e=1}^{n_{el}} \Gamma^e - \Gamma. \quad (9)$$

Let  $\mathcal{V}^h \subset H^1(\Omega)$  denote the space of weighting functions. We assume  $\mathcal{V}^h$  consists of typical  $C^0$  finite element interpolation functions and that if  $w^h \in \mathcal{V}^h$ , then

$$w^h(\mathbf{x}) = 0, \quad \forall \mathbf{x} \in \Gamma_g. \quad (10)$$

Let  $\mathcal{S}_t^h \subset H^1(\Omega)$  denote the set of trial solutions. We also assume  $\mathcal{S}_t^h$  consists of typical  $C^0$  finite element interpolation functions. Members  $\varphi^h(\cdot, t) \in \mathcal{S}_t^h$  may be decomposed as follows:

$$\varphi^h(\cdot, t) = v^h(\cdot, t) + g^h(\cdot, t), \quad (11)$$

where  $t \mapsto v^h(\cdot, t)$  is a curve in  $\mathcal{V}^h$  and  $g^h$  is a fixed extension of  $g$ , that is,

$$g^h(\mathbf{x}, t) = g(\mathbf{x}, t), \quad \forall \mathbf{x} \in \Gamma_g, \quad t \in ]0, T[. \quad (12)$$

We are interested in finding  $\varphi^h(\cdot, t) \in \mathcal{S}_t^h$ ,  $t \in [0, T]$ , such that, for all  $w^h \in \mathcal{V}^h$ :

$$\begin{aligned} & \int_{\Omega} (w^h \mathbf{a} \cdot \nabla \varphi^h + \nabla w^h \cdot \boldsymbol{\kappa} \nabla \varphi^h) d\Omega + \sum_{e=1}^{n_{el}} \int_{\Omega^e} \tau \mathbf{a} \cdot \nabla w^h (\varphi_{,t}^h + \mathbf{a} \cdot \nabla \varphi^h - \nabla \cdot \boldsymbol{\kappa} \nabla \varphi^h - f) d\Omega \\ &= \int_{\Omega} w^h (\dot{f} - \varphi_{,t}^h) d\Omega + \int_{\Gamma_h} w^h h d\Gamma \end{aligned} \quad (13)$$

and

$$0 = \int_{\Omega} w^h (\varphi^h|_{t=0} - \varphi_0) d\Omega. \quad (14)$$

**REMARK 2.1.** Equation (13) is the variational equation of the semidiscrete SUPG method. This form of the equation first appeared in [9]. Note that the sum of integrals over element interiors cannot be written as a global integral over  $\Omega$  due to the presence of the term  $\nabla \cdot \boldsymbol{\kappa} \nabla \varphi^h$ .

The Euler–Lagrange form of the variational equation is revealing. To obtain it we need to integrate by parts:

$$\begin{aligned}
0 = & \sum_{e=1}^{n_{el}} \int_{\Omega^e} \tilde{w}^h (\underbrace{\varphi_{,t}^h + \mathbf{a} \cdot \nabla \varphi^h - \nabla \cdot \boldsymbol{\kappa} \nabla \varphi^h - f}_{\text{advection-diffusion equation residual}}) d\Omega \\
& + \int_{\Gamma_{int}} w^h [\underbrace{\mathbf{n} \cdot \boldsymbol{\kappa} \nabla \varphi^h}_{\text{diffusive-flux continuity condition residual}}] d\Gamma + \int_{\Gamma_h} w^h (\underbrace{\mathbf{n} \cdot \boldsymbol{\kappa} \nabla \varphi^h - h}_{\text{diffusive-flux boundary condition residual}}) d\Gamma,
\end{aligned} \tag{15}$$

where

$$\tilde{w}^h = w^h + \tau \mathbf{a} \cdot \nabla w^h \tag{16}$$

and

$$\begin{aligned}
[\mathbf{n} \cdot \boldsymbol{\kappa} \nabla \varphi^h](\mathbf{x}, t) &= \mathbf{n}(\mathbf{x}) \cdot \{(\boldsymbol{\kappa} \nabla \varphi^h)(\mathbf{x}^+, t) - (\boldsymbol{\kappa} \nabla \varphi^h)(\mathbf{x}^-, t)\} \\
&= \mathbf{n}^+(\mathbf{x}) \cdot (\boldsymbol{\kappa} \nabla \varphi^h)(\mathbf{x}^+, t) + \mathbf{n}^-(\mathbf{x}) \cdot (\boldsymbol{\kappa} \nabla \varphi^h)(\mathbf{x}^-, t).
\end{aligned} \tag{17}$$

The meaning of the ‘+’ and ‘-’ superscripts in (17) is illustrated in Fig. 1.

**REMARKS 2.2.** (1) If  $\tau = 0$ , the above formulation reduces to the standard Galerkin finite element method.

(2) C. Johnson and his associates have shown that the most appropriate generalization of the SUPG concept to time-dependent phenomena involves a fully-discrete space-time formulation. For steady problems, both the fully-discrete and semidiscrete formulations coincide.

(3) Note that SUPG constitutes a *residual* method. That is, if  $\varphi^h \leftarrow \varphi$ , the exact solution, then (13) is still satisfied. This can be clearly seen from the Euler-Lagrange form of the variational equation, namely (15).

### 2.3. Error estimates

Consider the steady case in which  $f$ ,  $g$  and  $h$  are no longer time-dependent,  $\varphi_{,t} = 0$ , and the initial condition is dropped. Appropriate selection of  $\tau$  leads to the following error estimate (see [15, 16, 19]):

$$\alpha_{\max}^{-1} \|\nabla e\|_{L_2}^2 + ch^{-1} \|e\|_{L_2}^2 + \|\hat{\mathbf{a}} \cdot \nabla e\|_{L_2}^2 \leq Ch^{2k} (1 + \alpha_{\max}^{-1}) \|\varphi\|_{H^{k+1}}^2, \tag{18}$$

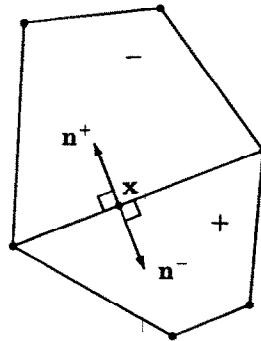


Fig. 1.

where  $e = \varphi^h - \varphi$  is the error;  $h$  is the mesh parameter;  $\|\cdot\|_{L_2}$  denotes the  $L_2$  norm;  $\|\cdot\|_{H^{k+1}}$  denotes the Sobolev norm of order  $k+1$ ; the index  $k$  is the degree of the complete polynomial present in the element interpolation functions;  $\hat{a} = a/|a|_2$  where  $|a|_2 = (a \cdot a)^{1/2}$ ;  $c$  and  $C$  are constants;

$$\alpha_{\max} = \max_e (\alpha_{\max}^e), \quad (19)$$

$$\alpha_{\max}^e = \sup_{x \in \Omega^e} \left( \frac{1}{2} |a|_2 h^e / \kappa \right), \quad (20)$$

in which  $h^e$  is the mesh parameter for the  $e$ th element.

**REMARKS 2.3.** (1) If  $\alpha_{\max} \gg 1$  (i.e., the advection-dominated case), then

$$\|\hat{a} \cdot \nabla e\|_{L_2} = O(h^k), \quad (21)$$

$$\|e\|_{L_2} = O(h^{k+1/2}). \quad (22)$$

The error in the streamline derivative, (21), is of optimal order. The theoretical  $L_2$  error, (22), is suboptimal exhibiting ‘gap’ equal to  $1/2$ . Numerical studies [19] suggest the  $L_2$  error may actually be optimal (i.e.  $O(h^{k+1})$ ) in many cases in which the exact solution is sufficiently smooth.

(2) If  $\alpha_{\max} \ll 1$  (i.e., the diffusion-dominated case), then

$$\|\nabla e\|_{L_2} = O(h^k). \quad (23)$$

A standard duality argument may be employed in this case to show also that

$$\|e\|_{L_2} = O(h^{k+1}). \quad (24)$$

(3) In the advection-dominated case in which sharp internal or boundary layers are present, SUPG attains the error estimates (21) and (22) *locally*, that is, outside a small neighborhood containing the layer. This may be contrasted with the standard Galerkin finite element method in which the presence of sharp layers globally vitiates the solution. The improved behavior of SUPG in the presence of sharp layers may be attributed to the additional stability of the method engendered by control of the streamline gradient. Nevertheless, some oscillations remain due to the absence of control of gradients in directions other than the streamline.

(4) In order to prove the results quoted above,  $\tau$  must be selected elementwise to satisfy the following minimal conditions: if  $\alpha_{\max}^e$  is small, then

$$\tau^e \leq c_1 (h^e)^2 / \kappa, \quad (25)$$

and, if  $\alpha_{\max}^e$  is large, then

$$\tau^e = c_2 h^e / |a|_2, \quad (26)$$

where  $c_1$  and  $c_2$  are nondimensional constants which depend upon element type. Precise computational formulae for  $\tau^e$  are presented in Appendix A.

### 3. Discontinuity capturing

Let  $\mathbf{a}_{\parallel}$  denote the projection of  $\mathbf{a}$  onto  $\nabla\varphi^h$ , that is,

$$\mathbf{a}_{\parallel} = \begin{cases} \frac{(\mathbf{a} \cdot \nabla\varphi^h)}{|\nabla\varphi^h|^2} \nabla\varphi^h, & \text{if } \nabla\varphi^h \neq 0, \\ 0, & \text{if } \nabla\varphi^h = 0. \end{cases} \quad (27)$$

Note that  $\mathbf{a}_{\parallel}$  is a homogeneous function of degree zero in  $\nabla\varphi^h$ . Let

$$\mathbf{a}_{\perp} = \mathbf{a} - \mathbf{a}_{\parallel}. \quad (28)$$

The set-up is illustrated in Fig. 2. A simple, but important, result is that

$$\mathbf{a}_{\parallel} \cdot \nabla\varphi^h = \mathbf{a} \cdot \nabla\varphi^h. \quad (29)$$

This suggests a way of developing an improved method. Namely, in place of (16), let

$$\tilde{w} = w^h + \tau_1 \mathbf{a} \cdot \nabla w^h + \tau_2 \mathbf{a}_{\parallel} \cdot \nabla w^h. \quad (30)$$

Employing (30) in (15) and using (29) illustrates that improved stability is achieved. The important terms to consider are those which represent the interaction of (30) with  $\mathbf{a} \cdot \nabla\varphi^h$  in (15), viz.

$$\tilde{w}^h (\cdots + \mathbf{a} \cdot \nabla\varphi^h + \cdots) = \cdots + w^h \mathbf{a} \cdot \nabla\varphi^h + \nabla w^h \cdot \underbrace{\tau_1 \mathbf{a} \mathbf{a}^t \nabla\varphi^h}_{\text{streamline operator}} + \nabla w^h \cdot \underbrace{\tau_2 \mathbf{a}_{\parallel} \mathbf{a}_{\parallel}^t \nabla\varphi^h}_{\text{discontinuity-capturing operator}} + \cdots. \quad (31)$$

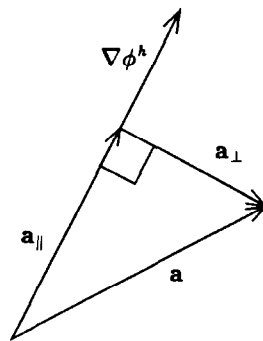


Fig. 2.

The last term engenders control over gradients in the direction  $\nabla\varphi^h$ . The additional term significantly increases the robustness of SUPG in the presence of sharp layers. The price that one pays for this improvement is that the new method—SUPG plus discontinuity capturing—is always *nonlinear* in that  $a_{||}$  depends upon  $\nabla\varphi^h$ .

**REMARK 3.1.** Davis [61] has developed a finite difference method for the compressible Euler equations in which the difference equations align themselves perpendicular to steep gradients in the discrete solution. The discontinuity-capturing term developed herein is seen to automatically create a similar effect.

#### 4. Numerical results

All results were run on a VAX 11-780 in single precision (32 bits per single-precision word). The calculations all involve steady flows. An explicit forward-Euler time-stepping scheme was used and the calculations proceeded until a steady state was achieved. The following procedures were compared:

- (i) *Streamline-upwind/Petrov–Galerkin* (SUPG).
- (ii) *SUPG plus discontinuity capturing* (DC1). In this case,  $\tau_1 = \tau$  and  $\tau_2 = \tau_{||}$  (see Appendix A).
- (iii) *SUPG plus discontinuity-capturing* (DC2). In this case,  $\tau_1 = \tau$  and  $\tau_2 = \max(0, \tau_{||} - \tau)$ . For the square elements employed  $\tau_{||} \geq \tau$  (see Appendix A).
- (iv) *Mizukami–Hughes scheme* (MH). This method is described in [18]. In this case the elements are triangular.

For methods (i)–(iii), square bilinear elements were employed with  $2 \times 2$  quadrature. In the formulae for the  $\tau$  given in Appendix A, the  $p$ -norm is employed (i.e.,  $|\cdot|_p$ ). Numerical results are presented for  $p = 2$  and  $p = \infty$  (i.e., the max norm).

##### 4.1. Advection skew to the mesh with downwind essential boundary conditions

This is a very difficult set of problems which severely tests the robustness of a method. The physical diffusivity is assumed to be very small in the sense that the element Peclet number is very large. A  $20 \times 20$  square mesh was employed. In each case considered the inflow boundary data are discontinuous resulting in an internal layer skew to the mesh. In addition, in two cases there are two boundary layers which intersect at a corner. In the third case there is one boundary layer. Results for the various methods are compared with nodally-exact solutions interpolated via piecewise-bilinear finite element shape functions. The exact solutions are labelled with an ‘E’. Problems of this type were first considered in [8]. It may be noted that results for a Galerkin formulation are wildly oscillatory for these test cases (not shown).

In Fig. 3 all the methods are compared with the exact solution. The value of  $p$  used for cases (i)–(iii) was  $\infty$  (i.e., the max norm). SUPG typically produces oscillations about the internal layer, and produces a particularly noticeable oscillation about one of the boundary layers. The effect of the discontinuity-capturing term is apparent. For DC1, all layers are considerably smoothed out compared with SUPG. Nevertheless, the solution is still quite good with all layers and plateaus being clearly apparent. The less diffusive DC2 produces sharper layers



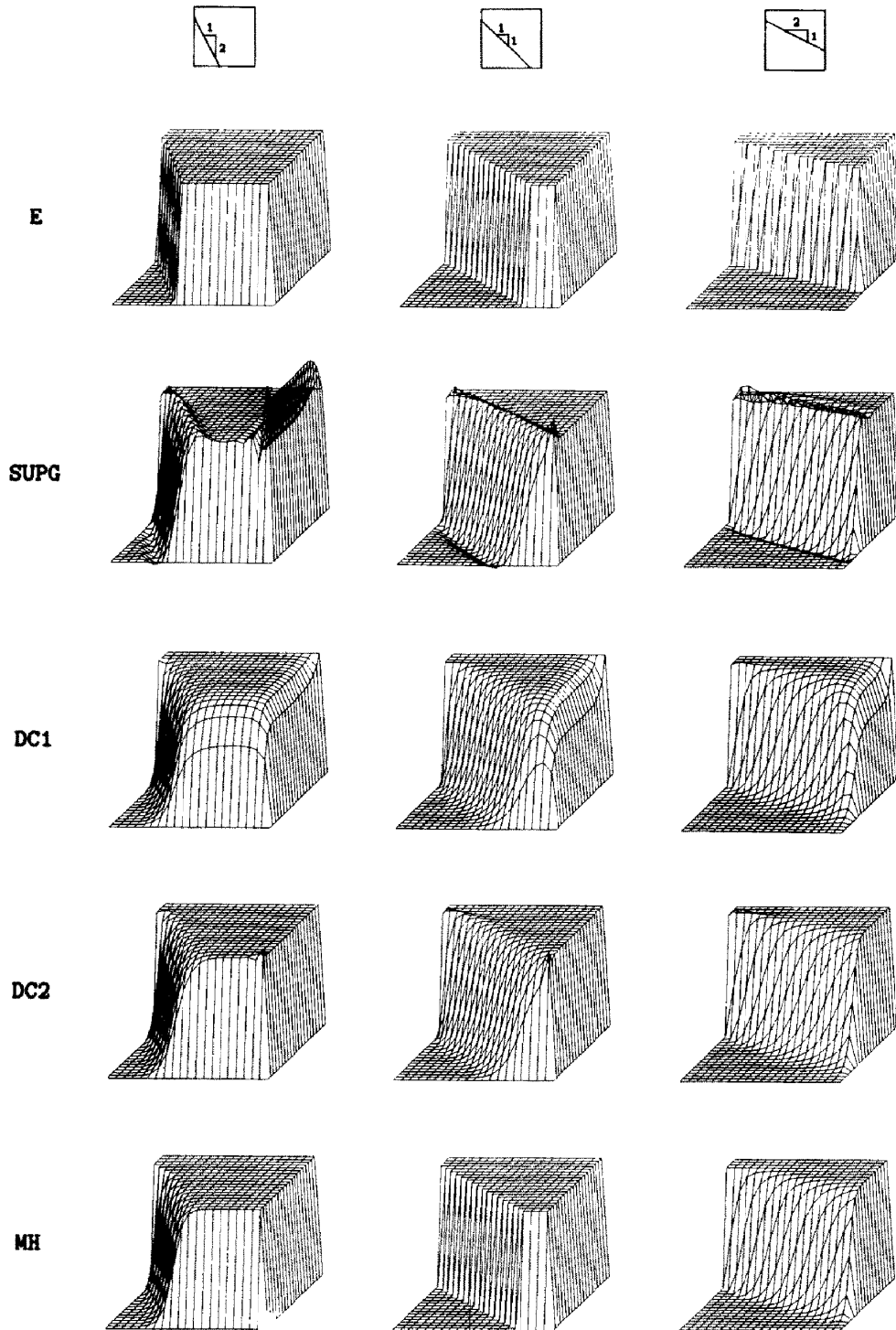


Fig. 3. Advection skew to the mesh. Comparison of results. Methods SUPG, DC1 and DC2 employ  $p = \infty$  in the definition of the  $\tau$ .

than DC1, as expected. There are a few nodes for DC2 which exhibit some overshoot. However, the significant improvement of DC1 and DC2 over SUPG is manifest. Each square is decomposed into two triangles for MH. The diagonals of the triangles are oriented to be roughly parallel to the internal layer. The monotonicity and high precision of the MH scheme are self-evident. Crisp resolution of the internal layers and exact capturing of the boundary layers is attained. In the case in which the flow is at 45 degrees to the mesh, the results are nodally exact.

In Fig. 4, calculations are presented for methods (i)–(iii) in which  $p = 2$  was employed (i.e., the 2-norm). The results for  $p = 2$  are somewhat less diffusive than for  $p = \infty$  as may be verified by comparing Figs. 3 and 4. Thus SUPG with  $p = 2$  is even more oscillatory than SUPG with  $p = \infty$ . On the other hand, DC1 with  $p = 2$  is somewhat crisper and improved compared with  $p = \infty$ . The overshoot exhibited at certain nodes by DC2 with  $p = \infty$  is somewhat increased for  $p = 2$ . It turns out that in generalizing the present methodology to multidimensional systems, the analog of the 2-norm is much more convenient to calculate than the analog of the max norm.

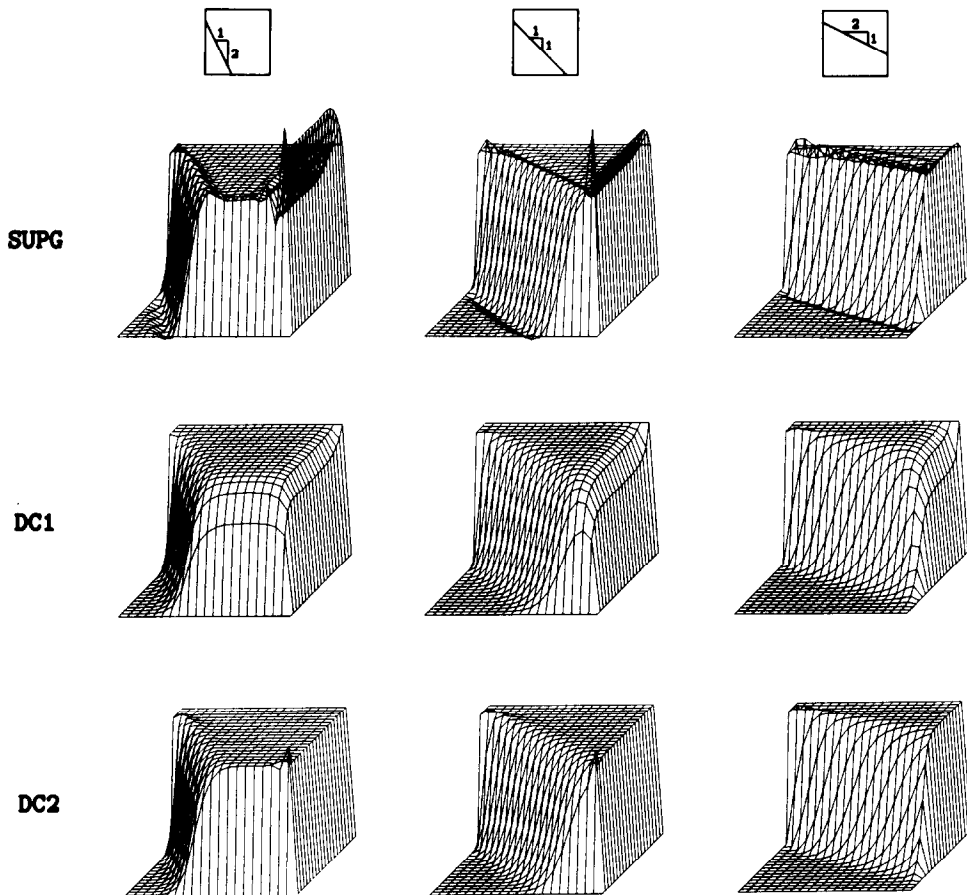


Fig. 4. Advection skew to the mesh. Comparison of results for  $p = 2$ .

#### 4.2. Advection in a rotating flow field ('donut problem')

This problem was also first considered in [8] which may be consulted for a detailed description. The flow field is defined by

$$a_1 = -x_2, \quad a_2 = x_1. \quad (32)$$

Results are presented for a  $30 \times 30$  square mesh. For this problem, results using the max norm are virtually indistinguishable from those for the 2-norm. Consequently, only one set of calculations, for the 2-norm, are shown. The results for SUPG are nearly exact and thus may be taken as a reference. The results for DC1 and DC2 are almost identical, registering a maximum relative amplitude error of about 10 percent. The result for MH is similar, but slightly better, in that the maximum amplitude error is about 6 percent. This problem is a good test of accuracy and it is felt that all the methods compared behaved quite well. It may be mentioned in way of contrast that classical upwind differences produce 70 percent amplitude error for this problem due to excessive crosswind diffusion (see [8]).

**REMARK 4.1.** Note that the gradient in the exact solution of the donut problem points in the radial direction and thus is perpendicular to  $\mathbf{a}$ . It may be noted, however, that the presence of the discontinuity-capturing operator clearly does not engender excessive crosswind diffusion. The reason for this can be seen as follows: let  $\theta$  denote the included angle between  $\mathbf{a}$  and  $\nabla\phi^h$ . By the definition of  $\mathbf{a}_{\parallel}$  we have that

$$|\mathbf{a}_{\parallel}|_2 = (\cos \theta) |\mathbf{a}|_2. \quad (33)$$

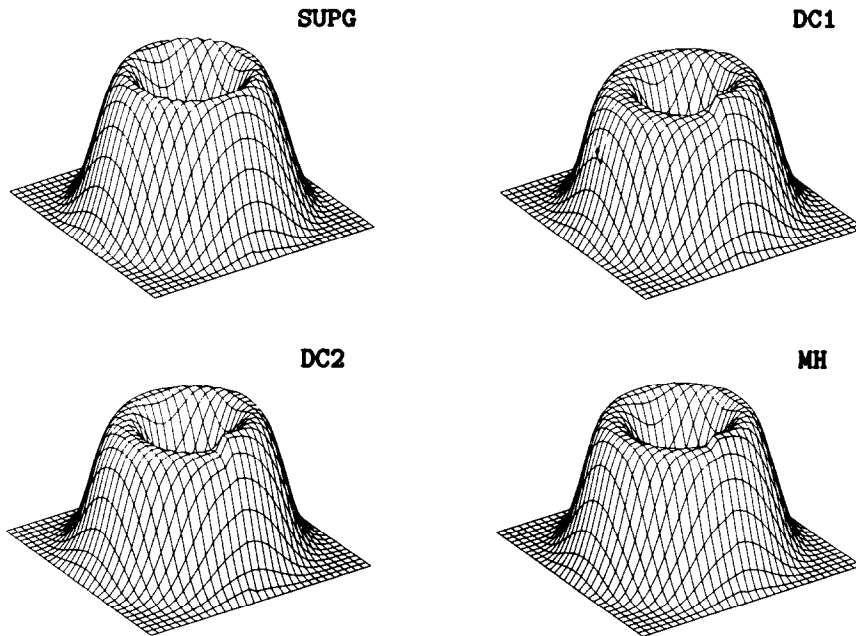


Fig. 5. Advection in a rotating flow field. Comparison of results. Methods SUPG, DC1 and DC2 employ  $p = 2$  in the definition of the  $\tau$ .

The angle,  $\psi$ , by which  $\mathbf{a}$  and  $\nabla\varphi^h$  fail to be perpendicular is

$$\psi = \frac{1}{2}\pi - \theta. \quad (34)$$

Let  $\varepsilon$  denote the absolute value of  $\psi$ . An estimate of the magnitude of the discontinuity-capturing operator is easily calculated, viz.

$$\frac{|\tau_2 \mathbf{a}_\parallel \mathbf{a}_\parallel^\dagger|_2}{|\tau_1 \mathbf{a} \mathbf{a}^\dagger|_2} = O(\varepsilon), \quad (35)$$

where, in (35),  $|\cdot|_2$  denotes the matrix 2-norm. Thus the effect of the discontinuity-capturing term is very small when  $\mathbf{a}$  and  $\nabla\varphi^h$  are nearly perpendicular.

## 5. Conclusions

In this paper we have addressed the main deficiency of SUPG, namely the tendency to produce oscillations about sharp internal and boundary layers. We have shown that a term may be added to the weighting function which enables control to be exercised over sharp gradients. This so-called ‘discontinuity-capturing term’ depends on the direction of the gradient in the discrete solution and thus the method is *nonlinear* even for linear problems. Numerical results for problems with sharp layers illustrate the beneficial effects of the new term.

## Appendix A. Formulae for $\tau$

### A.1. Determination of $\tau$

Let  $\mathbf{x}^\varepsilon = \mathbf{x}^\varepsilon(\xi)$  denote the geometric mapping from the parent domain to  $\Omega^\varepsilon \subset \mathbb{R}^{n_{sd}}$ . The inverse mapping is written  $\xi^\varepsilon = \xi^\varepsilon(\mathbf{x})$ . The procedure for selecting  $\tau$  that we currently favor derives all relevant quantities from a vector  $\mathbf{b}^\varepsilon$  defined as

$$\mathbf{b}^\varepsilon = (\mathbf{a} \cdot \nabla) \xi^\varepsilon, \quad (A.1)$$

or in components,

$$b_i^\varepsilon = a_j \frac{\partial \xi_i^\varepsilon}{\partial x_j}. \quad (A.2)$$

The ‘length’ of  $\mathbf{b}^\varepsilon$  with respect to the  $p$ -norm is denoted

$$|\mathbf{b}^\varepsilon|_p = \left( \sum_{i=1}^{n_{sd}} |b_i^\varepsilon|^p \right)^{1/p}. \quad (A.3)$$

An element mesh parameter may be defined by

$$\frac{1}{2}h^e = |\mathbf{a}|_2/|\mathbf{b}^e|_p. \quad (\text{A.4})$$

Note that  $h^e = h^e(\mathbf{x})$ ,  $\mathbf{x} \in \Omega^e$ . The element Peclet number is defined as

$$\alpha^e = \frac{1}{2}|\mathbf{a}|_2 h^e / \kappa. \quad (\text{A.5})$$

A nondimensional numerical diffusivity,  $\tilde{\xi}^e = \tilde{\xi}(\alpha^e)$ , may be defined by any of the following formulae:

$$\tilde{\xi}(\alpha^e) = \begin{cases} c_2 \left( \coth \left( \frac{c_1 \alpha^e}{c_2} \right) - \left( \frac{c_1 \alpha^e}{c_2} \right)^{-1} \right) & \text{('optimal', [5])}, \\ \min \left( \frac{c_1 \alpha^e}{3}, c_2 \right) & \text{('doubly asymptotic', [8])}, \\ \max \left( 0, c_2 - \left( \frac{c_1 \alpha^e}{c_2} \right)^{-1} \right) & \text{('critical', [5])}, \end{cases} \quad (\text{A.6})$$

where  $c_1$  and  $c_2$  are constants which depend on the particular type of element being employed. For example, for linear elements in one dimension, bilinear elements in two dimensions, and trilinear elements in three dimensions, values of  $c_1 = c_2 = 1$  are effective. Note that, in all cases, as  $\alpha^e \rightarrow \infty$ ,  $\tilde{\xi}^e \rightarrow c_2$ . The dimensional numerical diffusivity is given by

$$\kappa^e = \frac{1}{2}|\mathbf{a}|_2 h^e \tilde{\xi}^e \quad (\text{A.7})$$

and, finally,  $\tau^e$  may be expressed as

$$\tau^e = \frac{\bar{\kappa}^e}{|\mathbf{a}|_2^2} = \frac{h^e}{2|\mathbf{a}|_2} \tilde{\xi}^e = \frac{\tilde{\xi}^e}{|\mathbf{b}^e|_p}. \quad (\text{A.8})$$

It is important to realize that all of (A.1)–(A.8) are *functions* of  $\mathbf{x} \in \Omega^e$ .

#### A.2. Determination of $\tau_{\parallel}$

Corresponding to (A.1)–(A.8) we have

$$\mathbf{b}_{\parallel}^e = (\mathbf{a}_{\parallel} \cdot \nabla) \xi^e, \quad (\text{A.9})$$

$$\frac{1}{2}h_{\parallel}^e = |\mathbf{a}_{\parallel}|_2/|\mathbf{b}_{\parallel}^e|_p, \quad (\text{A.10})$$

$$\alpha_{\parallel}^e = \frac{1}{2}|\mathbf{a}_{\parallel}|_2 h_{\parallel}^e / \kappa, \quad (\text{A.11})$$

$$\tilde{\xi}_{\parallel}^e = \tilde{\xi}(\alpha_{\parallel}^e), \quad (\text{A.12})$$

$$\kappa_{\parallel}^e = \frac{1}{2}|\mathbf{a}_{\parallel}|_2 h_{\parallel}^e / \kappa, \quad (\text{A.13})$$

$$\tau_{\parallel}^e = \frac{\tilde{\kappa}_{\parallel}^e}{|\mathbf{a}_{\parallel}|_2^2} = \frac{1}{2} h_{\parallel}^e \tilde{\xi}_{\parallel}^e / |\mathbf{a}_{\parallel}|_2 = \frac{\tilde{\xi}_{\parallel}^e}{|\mathbf{b}_{\parallel}^e|_p}. \quad (\text{A.14})$$

### A.3. Determination of $\tau_1$ and $\tau_2$

We have experimented with two sets of values of the parameters:

(i) The first and perhaps most obvious choice for the parameters is

$$\tau_1^e = \tau^e, \quad \tau_2^e = \tau_{\parallel}^e. \quad (\text{A.15})$$

The drawback to (A.15) is apparent when  $\mathbf{a}_{\parallel} = \mathbf{a}$ . In this case an effective doubling of  $\tau^e$  is engendered. This can be circumvented by the following alternative.

(ii) This choice seeks to avoid the doubling effect of (A.15) by removing the component of  $\tau^e \mathbf{a} \mathbf{a}^t$  in the direction  $\mathbf{a}_{\parallel} \mathbf{a}_{\parallel}^t$ . We take

$$\tau_1^e = \tau^e, \quad \tau_2^e = \max(0, \tau_{\parallel}^e - \tau^e). \quad (\text{A.16})$$

The 'max' function is used in the above to guard against  $\tau_{\parallel}^e - \tau^e$  becoming negative, which can occur for distorted element geometries.

## References

- [1] J.H. Argyris, J.St. Doltsinis, P.M. Pimenta and H. Wüstenberg, Natural finite element techniques for viscous fluid motion, *Comput. Meths. Appl. Mech. Engrg.* 45 (1984) 3–55.
- [2] A.N. Brooks and T.J.R. Hughes, Streamline upwind/Petrov–Galerkin methods for advection dominated flows, in: *Proceedings Third International Conference on Finite Element in Fluid Flows*, Banff, Canada, 1980.
- [3] A.N. Brooks and T.J.R. Hughes, Streamline upwind/Petrov–Galerkin formulations for convection dominated flows with particular emphasis on the incompressible Navier–Stokes equations, *Comput. Meths. Appl. Mech. Engrg.* 32 (1982) 199–259.
- [4] G.F. Carey and J.T. Oden, *Proceedings Fifth International Symposium on Finite Elements and Flow Problems*, University of Texas, Austin, TX, U.S.A., 1984.
- [5] I. Christie, D.F. Griffiths, A.R. Mitchell and O.C. Zienkiewicz, Finite element methods for second order differential equations with significant first derivatives, *Internat. J. Numer. Meths. Engrg.* 10 (1976) 1389–1396.
- [6] S.F. Davis, A rotationally biased upwind difference scheme for the Euler equations, *J. Comput. Phys.* 56 (1984) 65–92.
- [7] M.D. Huang, Constant-flow patch test—a unique guideline for the evaluation of discretization schemes for the current continuity equations (1985) to appear.
- [8] T.J.R. Hughes and A.N. Brooks, A multidimensional upwind scheme with no crosswind diffusion, in: T.J.R. Hughes, ed., *Finite Element Methods for Convection Dominated Flows* (ASME, New York, 1979) 19–35.
- [9] T.J.R. Hughes and A.N. Brooks, A theoretical framework for Petrov–Galerkin methods with discontinuous weighting functions: application to the streamline upwind procedure, in: R.H. Gallagher, D.H. Norrie, J.T. Oden and O.C. Zienkiewicz, *Finite Elements in Fluids*, Vol. IV (Wiley, London, 1982) 46–65.
- [10] T.J.R. Hughes, M. Mallet, Y. Taki, T. Tezduyar and R. Zanutta, A one dimensional shock capturing finite element method and multidimensional generalizations, in: *Proceedings Workshop on Numerical Methods for the Compressible Euler Equations*, INRIA, Rocquencourt, December 1983 (SIAM, Philadelphia, PA, 1985).
- [11] T.J.R. Hughes and T.E. Tezduyar, Finite element methods for first-order hyperbolic systems with particular emphasis on the compressible Euler equations, *Comput. Meths. Appl. Mech. Engrg.* 45 (1984) 217–284.

- [12] T.J.R. Hughes, T.E. Tezduyar and A.N. Brooks, A Petrov–Galerkin finite element formulation for systems of conservation laws with special references to the compressible Euler equations, in: K.W. Morton and M.J. Baines, eds., *Numerical Methods for Fluid Dynamics* (Academic Press, London, 1982) 97–125.
- [13] T. Ikeda, Maximum Principle in Finite Element Models for Convection-Diffusion Phenomena (North-Holland, Amsterdam, 1983).
- [14] C. Johnson, Finite element methods for convection-diffusion problems, in: R. Glowinski and J.L. Lions, eds., *Computer Methods in Engineering and Applied Sciences*, Vol. V (North-Holland, Amsterdam, 1982).
- [15] C. Johnson, Streamline diffusion methods for problems in fluid mechanics, in: *Finite Elements in Fluids*, Vol. VI (Wiley, London, 1985).
- [16] C. Johnson, U. Nävert and J. Pitkäranta, Finite element methods for linear hyperbolic problem, *Comput. Meths. Appl. Mech. Engrg.* 45 (1984) 285–312.
- [17] C. Johnson and J. Saranen, Streamline diffusion methods for the incompressible Euler and Navier–Stokes equations, *Math. Comp.*, to appear.
- [18] A. Mizukami and T.J.R. Hughes, A Petrov–Galerkin finite element method for convection-dominated flows: an accurate upwinding technique for satisfying the maximum principle, *Comput. Meths. Appl. Mech. Engrg.* 50 (1985) 181–193.
- [19] U. Nävert, A finite element methods for convection–diffusion problems, Ph.D. Thesis, Department of Computer Science, Chalmers University of Technology, Göteborg, Sweden, 1982.
- [20] J.G. Rice and R.J. Schnipke, A monotone streamline upwind finite element method for convection-dominated flows, *Comput. Meth. Appl. Mech. Engrg.* 48 (1985) 313–327.